Clinical simulations of prostate radiotherapy using BOMAB-like phantoms: Results for photons

Saveta Miljanić, Igor Bessières, jean-marc bordy, Francesco d'Errico, Angela Di Fulvio, Damian Kabat, Željka Knežević, Pawel Olko, Liliana Stolarczyk, Luigi Tana, et al.

AUTHOR QUERY FORM

ELSEVIER	**Journal:** RM **Article Number:** 4891	**Please e-mail or fax your responses and any corrections to:** **E-mail: corrections.esch@elsevier.tnq.co.in** **Fax: +31 2048 52789**

Dear Author,

Please check your proof carefully and mark all corrections at the appropriate place in the proof (e.g., by using on-screen annotation in the PDF file) or compile them in a separate list. Note: if you opt to annotate the file with software other than Adobe Reader then please also highlight the appropriate place in the PDF file. To ensure fast publication of your paper please return your corrections within 48 hours.

For correction or revision of any artwork, please consult http://www.elsevier.com/artworkinstructions.

Any queries or remarks that have arisen during the processing of your manuscript are listed below and highlighted by flags in the proof.

Location in article	Query / Remark: Click on the Q link to find the query's location in text Please insert your reply or correction at the corresponding line in the proof
Q1	References "Bordy et al., in this issue, d'Errico et al., in this issue, Harrison, in this issue, Knežević et al., in this issue" will be updated latter at the issue compilation stage.
Q2	Kindly update the reference "Lu et al., in press."
Q3	Please confirm that given names and surnames have been identified correctly.
Q4	For figure 10, the resolution is too low to be used. Please provide better quality figure of 300 dpi.
	Please check this box if you have no corrections to make to the PDF file ☐

Thank you for your assistance.

Radiation Measurements xxx (2013) 1–13

Contents lists available at SciVerse ScienceDirect

Radiation Measurements

journal homepage: www.elsevier.com/locate/radmeas

Clinical simulations of prostate radiotherapy using BOMAB-like phantoms: Results for photons

Q3 Saveta Miljanić [a,*], Igor Bessieres [b], Jean-Marc Bordy [c], Francesco d'Errico [d], Angela di Fulvio [d], Damian Kabat [e], Željka Knežević [a], Pawel Olko [f], Liliana Stolarczyk [f], Luigi Tana [g], Roger Harrison [h]

[a] Ruđer Bošković Institute, Bijenička c. 54, 10000 Zagreb, Croatia
[b] CEA, LIST, DCSI, 91191 Gif sur Yvette, France
[c] CEA, LIST, LNE/LNHB, 91191 Gif sur Yvette, France
[d] Department of Mechanical, Nuclear and Production Engineering, University of Pisa, Italy
[e] Centre of Oncology M. Skłodowska-Curie Memorial Institute, Krakow, Poland
[f] Institute of Nuclear Physics, Krakow, Poland
[g] University Hospital of Santa Chiara, Pisa, Italy
[h] University of Newcastle upon Tyne, Newcastle, UK

HIGHLIGHTS

- Dosimeters used (TLD, OSL and RPL) are suitable for out-of-field dosimetry.
- Generally agreement is within 3% compared with ion chamber reference measurements.
- Peripheral doses for the same PTV can vary by a factor of 4 for various modalities.
- Results revealed that the TPS used, regularly underestimated out-of-field doses.

ARTICLE INFO

Article history:
Received 17 April 2012
Received in revised form
28 July 2012
Accepted 14 December 2012

Keywords:
Out-of-field doses in radiotherapy
Photon dosimetry
RPL
TLD
OSL
IMRT
VMAT
Tomotherapy

ABSTRACT

In this part of work carried out by Working Group 9 (Radiation Protection Dosimetry in Medicine) of the European Radiation Dosimetry Group (EURADOS), water tank experiments described in this issue (Bordy et al., in this issue) were extended to a BOMAB-like phantom. This phantom is more clinically realistic than a water tank, sufficiently to allow the simulation of some clinical treatments. In the experiments to be described, four types of prostate treatment were simulated: Volumetric Modulated Arc Therapy (VMAT, 6 MV), Tomotherapy (6 MV), IMRT (6 MV and 18 MV), 5-field conformal radiotherapy (15 MV) and 4-field conformal radiotherapy (6 MV and 18 MV). Irradiations were performed in two centres, University Hospital of Santa Chiara, Pisa, Italy and Centre of Oncology M. Skłodowska-Curie Memorial Institute, Krakow, Poland. Whatever the difficulties and uncertainties in risk estimation, its foundation lies in the knowledge of the absorbed dose to the irradiated organs. Thus the measurement of out-of-field doses is a crucial pre-requisite for risk estimation and is the subject of the EURADOS Working Group 9. For photon out-of-field dose measurements TLD, OSL and RPL dosimeters were used. Comparison of dosimeters under the same irradiation conditions showed that dosimeters generally agreed to within 3% compared with ion chamber reference measurements. Other comparisons were possible with these data. They include a comparison of doses (beam profiles) in different positions in the BOMAB phantom, a comparison of different treatment modalities in the two contributing clinical centres (Pisa and Krakow) and a comparison of dose profiles resulting from the different treatment techniques and the corresponding doses calculated by the treatment planning systems used to generate the treatment plans. Finally, preliminary measurements of surface doses at selected points on the trunk of the BOMAB phantom were made using diode detectors. Comparison of out-of-field doses for different modalities in the two clinical centres shows that differences in out-of-field doses for the same Planning Treatment Volume (PTV) can be even a factor of 4. For sparing adjacent organs-at-risk the best results were obtained for IMRT. On the other hand the lowest out-of-field doses were for MLC conformal therapy.

* Corresponding author. Tel.: +385 1 4561053; fax: +385 1 4680 098.
E-mail address: saveta@irb.hr (S. Miljanić).

1350-4487/$ – see front matter © 2012 Published by Elsevier Ltd.
http://dx.doi.org/10.1016/j.radmeas.2012.12.012

1. Introduction

The greatest challenge for radiation therapy or any cancer therapy is to attain the highest probability of cure with the least morbidity. The simplest way in theory to increase this therapeutic ratio with radiation is to encompass all cancer cells with sufficient doses of radiation during each fraction, while simultaneously sparing surrounding normal tissues. The induction of cancers following radiotherapy (second cancers) has been known for many years although the estimation of the probability of radiation carcinogenesis is not straightforward. The overall cancer risk is influenced by the (usually non-uniform) dose to several radiosensitive organs distant from the radiotherapy target volume. Improvements in cancer treatment have increased survival times and thus increased incidence of second cancers may be expected in the future. In addition, increased whole body exposure may result from developments in radiotherapy. Starting with two-dimensional (2D) treatments, external radiotherapy consisted of a single beam from one to four directions. Beam setups were usually quite simple; plans frequently consisted of opposed lateral fields or fourfield "boxes". 3D conformal radiotherapy (3DCRT) is the term used to describe the design and delivery of radiotherapy treatment plans based on 3D image data with treatment fields individually shaped (advanced types use multi-leaf collimators (MLCs)) to treat only the target.

Conformal radiotherapy permits the delivery of a radical tumour dose while limiting the dose to normal tissue structures, thus minimising the adverse effects of treatment. As its name implies, Intensity-Modulated Radiation Therapy (IMRT) allows modulation of the intensity of each radiation beam, so that each field may have one or many areas of high intensity radiation and any number of lower intensity areas within the same field, thus allowing for greater control of the dose distribution with the target. In conjunction with Image-Guided Radiotherapy (IGRT) this approach should give better clinical results, with regard to both improved tumour control and sparing of organs-at-risk (OAR). On the other hand, increased whole body exposure may result (IAEA, 2008; Bucci et al., 2005). In addition, a variety of novel IMRT delivery methods have been investigated. One of these is Tomotherapy (or Helical Tomotherapy), in which the radiation is delivered slice-by-slice. Tomotherapy achieves higher spatial resolution than step-and-shoot IMRT, but requires longer delivery time and more monitor units (MUs) during daily treatment. As the number of MUs required for treatment delivery increases, so does the primary beam leakage dose (Mackie et al., 1993; Mutic and Low, 1998). Another approach, called "Volumetric Modulated Arc Therapy" (VMAT) proposed by Otto (2008) uses a dynamic modulated arc to deliver IMRT. The VMAT technology simultaneously coordinates gantry rotation, MLC motion, and dose rate modulation, facilitating highly conformal treatment and optimal sparing of the critical structures around the target (Pardo-Montero and Fenwick, 2009). VMAT appreciably reduces beam-on times in comparison with IMRT (Zhang et al., 2010). Recently there have been a number of published papers dealing with comparison of 3DCRT, IMRT and novel forms of IMRT: VMAT and Tomotherapy with regard to plan qualities and treatment efficiency for prostate cancer (Aoyama et al., 2006; Palma et al., 2008; Wolff et al., 2009; Aznar et al., 2010; Zhang et al., 2010; Tsai et al., 2011) and for other cancer types (Bertelsen et al., 2010; Viellot et al., 2010; Lee et al., 2011; Lu et al., in press). However, there are still insufficient data on the comparative measurement of out-of-field doses for these radiotherapy modalities and their influence on second cancer risk.

In the experiments to be described, four types of prostate treatment were simulated: VMAT, 6 MV, Tomotherapy (6 MV), IMRT (6 MV and 18 MV), 5-field conformal radiotherapy (15 MV) and 4-field conformal radiotherapy (6 MV and 18 MV). Irradiations were performed in two centres, University Hospital of Santa Chiara, Pisa, Italy and Centre of Oncology M. Skłodowska-Curie Memorial Institute, Krakow, Poland.

Whatever the difficulties and uncertainties in risk estimation, its foundation indisputably lies in the knowledge of the absorbed dose to the irradiated organs. Thus the measurement of out-of-field (sometimes referred to as peripheral) doses is a crucial prerequisite for risk estimation. Prostate treatments have been identified as a valuable benchmark for analysis by this Working Group. The prognosis for these patients (and those undergoing some other cancer treatments involving radiotherapy) has steadily improved (Harrison, in this issue; ~~this proceedings~~ according to CRUK, 2012). This means that an increasing number of patients will survive for periods comparable to or greater than the latent period (5 years–10 years or more) for expression of a second cancer, thus suffering a finite risk of carcinogenesis.

Dosimetry measurements were extended from water tank experiments to a BOMAB-like phantom. This phantom is more clinically realistic than a water tank, sufficiently to allow the simulation of some clinical treatments as it is composed of body, legs, arms and head sections in the form of water tanks of circular or elliptical cross section. The reason for using the BOMAB design was to have an intermediate phantom between a water tank and a realistic anthropomorphic phantom. It has the advantage of being "body" shaped, but its elliptical cross section makes it easier to model. Thus the results from this phantom are useful mainly for comparison with dose calculation algorithms (not for organ dose and risk estimates) and for comparison between dosimeters.

For photon dose measurements, thermoluminescence (TL), optically stimulated luminescence (OSL) and radiophotoluminescence (RPL) dosimeters were used. Dosimeters were first irradiated under the same irradiation conditions in a water tank and compared with ion chamber reference measurements. Other comparisons were possible with this data. They include a comparison of doses (beam profiles) in different positions in the BOMAB phantom, a comparison of different treatment modalities in the two contributing clinical centres (Pisa and Krakow) and a comparison of dose profiles resulting from the different treatment techniques and the corresponding doses calculated by the treatment planning systems used to generate the treatment plans. Finally, preliminary measurements of surface doses at selected points on the trunk of the BOMAB phantom were made using diode detectors. The aim is to investigate the possible relationships between surface doses and underlying doses within the phantom and thus to explore potential practical ways in which organ and tissue doses may be estimated when full-scale simulation is not possible in the clinic.

2. Material and methods

2.1. Treatment features

Treatment modalities for the clinical simulation of prostate therapy shown in Table 1 were performed mainly in two centres, University Hospital of Santa Chiara, Pisa, Italy and Centre of Oncology M. Skłodowska-Curie Memorial Institute, Krakow, Poland. Only Tomotherapy was performed in Campo di Marte Hospital in Lucca, Italy. For 15 MV 5-field MLC and 6 MV IMRT in Pisa, the treatment planning system (TPS) was a CMX XiO Rel. 4.40.05. For VMAT ("RapidArc" Varian implementation) a VARIAN Eclipse External beam Planning vers. 8.6 was used and for Tomotherapy (HI-ART TomoTherapy), a TomoHD treatment system – TomoDirect™ Treatment Delivery Mode. For 4-field MLC and IMRT

Please cite this article in press as: Miljanić, S., et al., Clinical simulations of prostate radiotherapy using BOMAB-like phantoms: Results for photons, Radiation Measurements (2013), http://dx.doi.org/10.1016/j.radmeas.2012.12.012

Table 1
Modalities of clinical simulation of prostate therapy.

Pisa	MU/	Krakow	MU/
Varian Clinac 2100 C	2 Gy	Varian Clinac 2300 CD	2 Gy
6 MV single 10 × 10 cm^2 field (ref)	251	6 MV single 10 × 10 cm^2 field (ref)	240
15 MV single 10 × 10 cm^2 field (ref)	218	18 MV single 10 × 10 cm^2 field (ref)	199
15 MV 5-field MLC	266	6 MV 4-field MLC	277
6 MV IMRT	432	18 MV 4-field MLC	218
6 MV VMAT (RapidArc)	481	6 MV IMRT	466
		18 MV IMRT	350
6 MV Tomotherapy	2495		

in Krakow, the TPS was Eclipse 8.6 (Varian). The value of monitor units in Table 1 for Tomotherapy has a different meaning than for the other modalities and is not actually comparable to the others.

The gantry angles were: 0, 270, 50, 90 and 310° for 5-field MLC in Pisa; 180, 45,103, 257 and 315° for IMRT in Pisa; 0, 75, 135, 255 and 285 for IMRT in Krakow and 0, 90,180, and 270° for 4-field MLC in Krakow. Reference beams (single 10 × 10 cm^2 fields) were used in Pisa (6 MV) and Krakow facilities (6 and 18 MV).

More details about treatments modalities are given in the paper by d'Errico et al. (in this issue).

All results in this paper are given for a dose of 2 Gy at the isocentre which is a commonly used fraction in radiation therapy.

2.2. BOMAB like phantom

The **BO**ttle **MA**nnikin **AB**sorber phantom was developed by Bush (1949) and has since been accepted in North America as the industry standard (ANSI, 1995) for calibrating whole body counting systems. A variation of this phantom was developed at the University of Pisa for this work (d'Errico et al., in this issue). It consists of a human trunk approximated by an ellipsoid, with cylinders representing the head, arms and legs. The phantom was constructed from Poly(methyl methacrylate) (PMMA), contains PMMA channels (pipes) to hold dosimeters, and is water-filled. It is sufficiently realistic to allow the simulation of some clinical treatments. The BOMAB phantom trunk is shown schematically in Fig. 1. Doses were measured in the BOMAB phantom over an axial distance of approximately 50 cm, at positions along five pipes, one on the longitudinal axis of the phantom and the remaining four adjacent and parallel. Rod elements 5 cm long with recesses for dosimeters were placed in the pipes. In the figure, the position of the planning treatment volume (PTV) is indicated (Only for OSL dosimeters distances between dosimeters were shorter in the PTV region). A BOMAB CT scan and simulated organs are shown in Fig. 2. We should emphasise some limitations of the "organ" dose concept using BOMAB phantom. These organs ("prostate", "bladder", "rectum") will receive scatter from the PMMA "lungs" whereas in reality we might expect these doses to be lower because of the decreased scatter from real lung. Also, positions and dimensions representing the rectum and bladder in the rods are only an approximation of the real organs. The organs' positions and dimensions were exactly the same in Pisa and Krakow irradiations but it was not possible to have exactly the same treatments plans. In Fig. 5 from the paper of Harrison (in this issue), the BOMAB phantom is shown as used for out-of-field dose measurements in a simulation of a prostate treatment.

2.3. Dosimetry methods used for photon dose measurements

Photon dosimetry methods applied in this work were thermoluminescence (TL), radiophotoluminescence (RPL) and optically stimulated luminescence (OSL). The basic principles of the methods, their characteristics, methods of their calibration and use were described in the paper by Knežević et al. (in this issue). Some data about these dosimetry methods relevant to the present work are also shown in Table 2. The following points are noteworthy:

(i) The dimensions and shape of dosimeters can influence their angular dependence. Special attention should be given for positions close to the target edge when a very sharp dose gradient exists.
(ii) Another important property is energy dependence of dosimeters. Dosimeters were calibrated in ^{60}Co field in terms of "absorbed dose to water" according to the procedure described in IAEA TRS 398 (2000). In the out-of-field region of the water tank exposed to endpoint energies of 6–20 MV there is a large contribution of scatter components with energies less than 0.2 MeV (Bordy et al., in this issue) for which

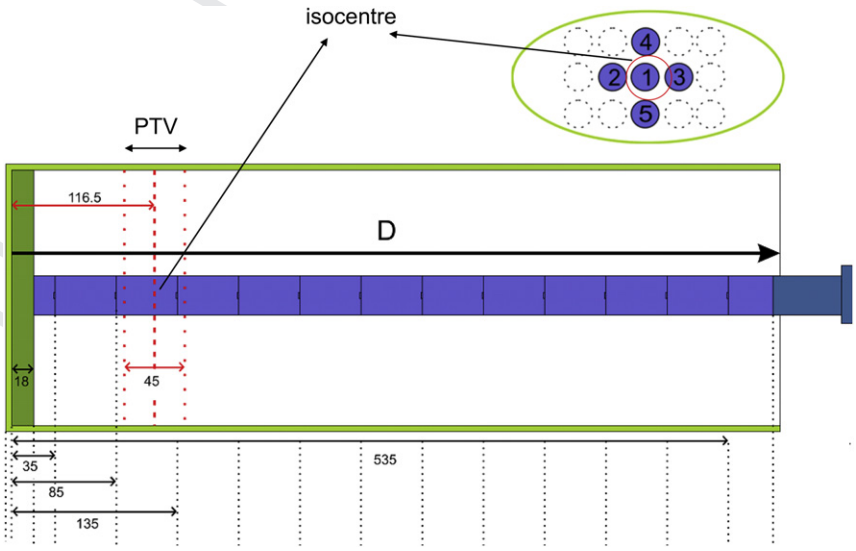

Fig. 1. Schematic diagram of the BOMAB phantom. A sagittal section through the central pipe (pipe 1) is shown. All dimensions are given in mm, length (D) is 600 mm, the planning treatment volume (PTV) is 45 mm.

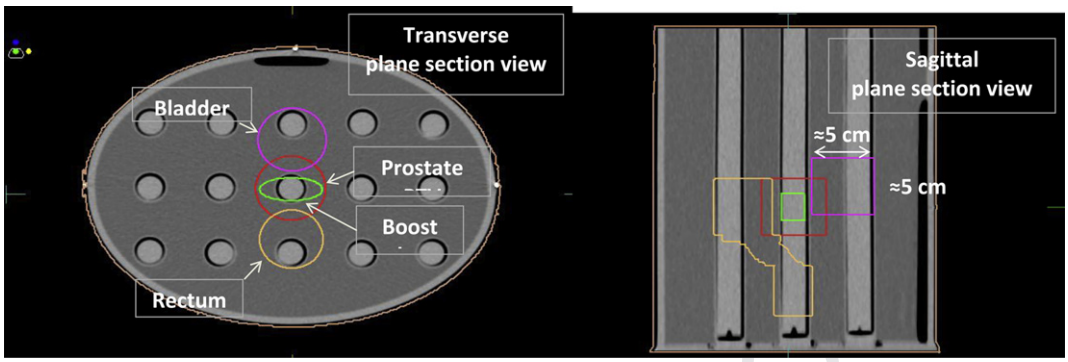

Fig. 2. BOMAB CT scan and simulated organs.

energy dependence of dosimeters could be different from that of water depending on the effective atomic number of the dosimeter material. It is well known that OSL dosimeter material and RPL glass overestimate dose in that energy range. For OSL, the response was corrected for spectra at different depths in water (Bordy et al., in this issue) whereas RPL type GD-352 M used in this work has a built-in Sn energy compensation filter. For both types of LiF:Mg, Ti TLDs used it was estimated that there is no need for applying any energy correction.

(iii) For endpoint energies greater than about 8 MV, there are dose contributions from fast neutrons from (γ, n) reactions in high-Z materials in the treatment head and the neutron sensitivity of photon dosimeters should be considered. The relative tissue kerma sensitivity, k_u, is defined as the ratio of the measured response of the dosimeter material to neutrons ($\eta_n K_{n,d}$) to the measured response to ^{60}Co gamma radiation ($\eta_s K_{s,d}$) relative to the tissue kerma for neutrons ($K_{n,t}$) and gamma radiation ($K_{s,t}$) respectively (ICRU, 1984; Gibson, 1986):

$$k_u = [(\eta_n K_{n,d})/K_{n,t}]/[(\eta_s K_{s,d})/K_{s,t})] \quad (1)$$

The neutron sensitivity depends not only on the composition of the detector material itself and on the cross sections of their constituents to different neutron spectra but also on the surrounding media. For irradiations in the BOMAB phantom, recoil protons from PMMA containing 8% hydrogen could be absorbed in dosimeters giving an increment of dose originating from neutron interactions in PMMA.

According to the manufacturer, the OSL detectors are insensitive to neutrons. Although there are data in the literature about responses of OSL to heavy charged particles (Sawakushi et al., 2008) these responses could be neglected due to low neutron dose component as discussed later.

For TLD-700 (^{7}LiF:Mg, Ti) it was found that relative neutron sensitivity, k_u, varies with neutron energies ranging from about 4% for Pu–Be neutrons (Krpan et al., 2008) to 7.5% for neutrons of 14.5 MeV (Miljanić et al., 2007). Concerning thermal neutrons, despite the fact that TLD-700 contains only a small amount of ^{6}LiF (~0.007% in mass) in the enriched ^{7}LiF, due to high cross section for the ^{6}Li (n,α)^{3}He reaction, response to the thermal neutrons cannot be neglected. The ratio of kerma factors of TLD-700 to tissue approximation for thermal neutrons is around 7 (ICRU, 1984) and the mean relative response, k_u, of 5.3 ± 3.4 was calculated from the seven cited papers (Gibson, 1986). This is a reason why special attention should be given to the response of TLD-700 to gamma radiation in the presence of thermal neutrons (Liu et al., 2001). Kry et al. (2005a) stated that in the energy range of neutrons around medical accelerators, TLD-700 is largely unresponsive to neutrons, detecting only about 1% of the neutron dose. Because the out-of-field neutron dose is typically of the order of 10% of the out-of-field photon dose, the neutron dose contribution produces only a 0.1% error in a measurement of photon dose under the conditions described in this paper. In their experiment neutron dose equivalent was determined by measuring the neutron fluence with activation foils and moderators. Thermal neutron fluence was measured using a bare gold foil suspended at the centre of the room (Kry et al., 2005a). They also concluded that the thermal neutrons

Table 2
Dosimetry methods used for photon dose measurements.

Institution	Dosimeter			
	Type	Dimensions (mm)	Energy dependence	Relative neutron sensitivity, k_u (Equation (1))
Commissariat à l'Énergie Atomique (CEA), Saclay	Optically stimulated luminescence (OSL)	Adapter: 10 × 10 × 2 Disc: φ 5 × 1	Corrected for spectra in different depths in water phantom	Insensitive (according to manufacturer)
Institute of Nuclear Physics (IFJ), Krakow	Thermoluminescence (TLD), type MTS-7 (^{7}LiF:Mg, Ti)	φ 4.5 × 0.9	Not corrected	The same as for TLD-700
Ruđer Bošković Institute (RBI), Zagreb	Radiophotoluminescence (RPL), type GD-352 M	Holder: φ 4.3 × 14.5 Rod: φ 1.5 × 12	Build-in Sn energy compensation filter	Thermal: 4.3 ± 0.1[a] Pu–Be: 0.032 ± 0.005[a] 14.5 MeV: 0.041 ± 0.005[a]
Ruđer Bošković Institute (RBI), Zagreb	Thermoluminescence (TLD), type TLD-700 (^{7}LiF:Mg, Ti)	φ 4.5 × 0.9	Not corrected	Thermal: 5.3 ± 3.4[b] Pu–Be: 0.041 ± 0.007[c] 14.5 MeV: 0.075 ± 0.003[d]

[a] Miljanić et al., 2008 (RPL type SC-1).
[b] Gibson, 1986.
[c] Krpan et al., 2008.
[d] Miljanić et al., 2007.

Please cite this article in press as: Miljanić, S., et al., Clinical simulations of prostate radiotherapy using BOMAB-like phantoms: Results for photons, Radiation Measurements (2013), http://dx.doi.org/10.1016/j.radmeas.2012.12.012

contribute less than 1% to the dose equivalent to the patient and in their work of dose calculations using a Monte Carlo model they included only those neutrons with energy greater than 0.6 eV (Kry et al., 2007). On the other hand, the results obtained by Vanhavere et al. (2004) showed that the thermal neutron component of the neutron dose increases from around 5% at 0 cm depth to around 40% at 10 cm depth in phantom but the total neutron doses decrease rapidly with the depth in phantom (contrary to the free-in-air situation). The calculation of photoneutron dose in soft tissue phantom irradiated by 25 MV X-ray was also performed by Agosteo et al. (1993). The default energy cuts of the code were considered for the transported particles, i.e. 1 keV and thermal energy for photons and neutrons, respectively. The maximum total photoneutron absorbed dose of 37 μGy/(X-ray therapy Gy) was found in the target volume of the four-field box irradiation phantom (Agosteo et al., 1993). This result would also give the negligible response of TLD-700 despite its high thermal neutron response in comparison to tissue.

For RPL, relative neutron sensitivity determined for type SC-1 is somewhat less than for TLD-700 as shown in Table 2 (according to Miljanić et al., 2008). The sensitivity of MTS-7 (^{7}LiF:Mg, Ti) should be very similar to that of TLD-700 (Knežević et al., in this issue).

2.4. Surface dose measurements

For surface dose measurements in University Hospital of Santa Chiara, Pisa, 8 diodes, QED (*p*-type silicon) blue detectors, produced by Sun Nuclear Corporation were used. Dimensions of the detectors were 0.8 × 0.8 cm^2, the sensitivity 32 nC/Gy, and the thickness of build-up material of 1.03 g/cm^2. Detectors were calibrated in a 6 MV beam (at a field size of 15 × 15 cm^2) in terms of absorbed dose to water by comparison with an ionisation chamber. During the irradiations, 4 diodes were placed on the anterior surface of the phantom trunk at distances of 10, 20, 30 and 40 cm from the transverse plane passing through the isocentre and 4 others were at the right lateral side of the trunk at distances 10, 20, 30 and 40 cm from the same plane. Due to relatively low diodes sensitivities, they were irradiated in two consecutive irradiations of BOMAB filled with dosimeters for certain modalities.

3. Results

3.1. Comparison of dosimetry systems

Prior to irradiations at reference clinical linac, dosimeters were calibrated in standard calibration conditions at ^{60}Co source as described in IAEA TRS 398 (2000). Then, dosimeters were compared in a reference clinical linac (Saturn 43) beam in a water tank at CEA-LIST/LNE LNHB, Saclay. Radiation qualities of 6, 12 and 20 MV were used. The reference calibration point in the water phantom was at a depth of 10 cm in water, on the central axis of the beam, field size was 10 × 10 cm^2. Doses were measured in the water tank over an axial distance of approximately 50 cm, at positions along a pipe (the beam axis was at 13.5 cm distance from the phantom inner wall).

Comparison of TLDs and RPL with a reference ionisation chamber (IC) is shown in Fig. 3 for all three radiation qualities. The mean ratios with standard deviations for doses in the out-of-field region in the range from 1.5 to 150 mGy were within 3%: (i) 6 MV: TLD/IC = 0.982 ± 0.027; RPL/IC = 0.976 ± 0.034, (ii) 12 MV: TLD/IC = 0.997 ± 0.025; RPL/IC = 1.029 ± 0.025, (iii) 20 MV: TLD/IC = 0.999 ± 0.046; RPL/IC = 1.027 ± 0.041. For 6 MV irradiations, TLD-100 (^{nat}LiF:Mg, Ti) from RBI was used instead of TLD-700. More details about irradiations and results at reference clinical linac are presented in the paper by Bordy et al. (in this issue).

In clinical irradiations in the BOMAB phantom the following dosimeters were used for dose distribution measurements: (i) Pisa: in all modalities (6 MV 1-field, 15 MV 5-field MLC, 6 MV IMRT, 6 MV VMAT and 6 MV tomotherapy) TLD MTS-7 and RPL were used. OSL was used in 15 MV 5-field MLC; (ii) Krakow: in all modalities (6 MV 1-field, 18 MV 1-field, 6 MV and 18 MV 4-field MLC, 6 MV and 18 MV IMRT) TLD MTS-7 was used, RPL and TLD-700 were used in 18 MV 1-field, 6 MV and 18 MV IMRT. OSL was used in 18 MV 4-field MLC. Results of the dosimeters comparison are shown for modalities where 3 types of dosimeters were irradiated: in Fig. 4 for 1-field 10 × 10 cm^2 in Krakow and 5-field MLC in Pisa, in Fig. 5 for 6 MV and 18 MV IMRT in Krakow. Doses are given for central "prostate" pipe (pipe 1). Variation of doses in the out-of-field region (above 1 mGy) was larger than in a water tank in the reference clinical linac beam: Standard deviations of groups of three dosimeters in all 5 pipes per modality were: 7%, 10%, 6% and 9% for 18 MV "reference" field (Krakow), 15 MV 5-field MLC (Pisa), 6 MV and 18 MV IMRT (Krakow), respectively.

3.2. Comparison of doses in different positions (pipes) in the phantom

Dose distribution measurements with OSL CEA dosimeters in 5 pipes are shown in Fig. 6: a) left: 5-field MLC, 15 MV, Pisa and b) right: 4-field MLC, 18 MV, Krakow. Pipe 1 corresponds to "prostate" and pipes 4 and 5 to "bladder" and "rectum", respectively. Pipes 2 and 3 are adjacent to the "prostate" pipe at the coronal plane. For irradiations by 5-field MLC, 15 MV in Pisa, the dose to "bladder" is 38.5% and in "rectum" 24.1% of that measured in "prostate". For irradiations by 4-field MLC, 18 MV, Krakow doses in "bladder" and "rectum" are 52,9% and 53,0% respectively of the "prostate" dose. Although doses in the treatment volumes for "prostate", "bladder" and "rectum" differ significantly, differences in out-of-field doses in different pipes do not show large differences.

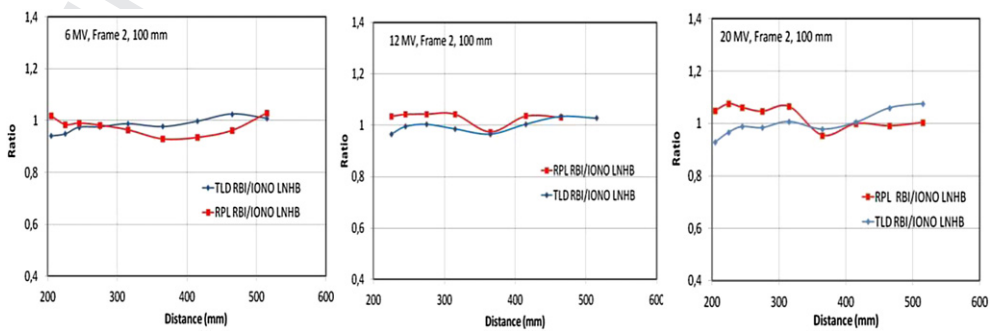

Fig. 3. Comparison of dosimeters in a reference clinical linac beam in a water tank at CEA-LIST/LNE LNHB, Saclay. IONO refers to ionisation chamber measurements.

Please cite this article in press as: Miljanić, S., et al., Clinical simulations of prostate radiotherapy using BOMAB-like phantoms: Results for photons, Radiation Measurements (2013), http://dx.doi.org/10.1016/j.radmeas.2012.12.012

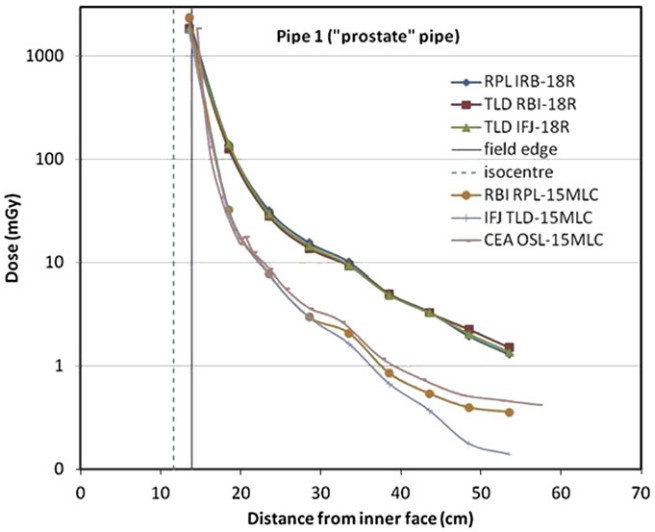

Fig. 4. Comparison of dosimeters irradiated in a BOMAB phantom by 18 MV 1-field 10 × 10 cm^2 (Krakow) and 15 MV 5-field MLC (Pisa).

3.3. Comparison of different treatment modalities

Comparison of out-of-field doses for different treatment modalities is shown in Fig. 7, a) for irradiations in Pisa and b) for irradiations in Krakow. Results are given for the central (prostate) pipe, for irradiations in Pisa mean values of RPL and TLD IFJ were used and for irradiations in Krakow results were obtained with TLD IFJ dosimeters. Without 1-field irradiations, the results show that the ratio of maximum (Tomotherapy) to minimum (15 MV 5-field MLC) doses ranging from 2.4 to 3.8 in Pisa and from 1.6 to 2.4 (the highest for 6 MV IMRT and the lowest for 18 MV 4-field MLC). For IMRT modalities there is a pronounced "hump" at about 20 cm distance from the isocentre origin from the head leakage (Ruben et al., 2011). The same effect is also visible for MLC but less pronounced. Generally, the lowest peripheral doses were obtained for MLC conformal therapy although comparing 18 MV IMRT and 18 MV 4-field MLC in Krakow, one can see that $D_{MLC}/D_{IMRT} > 1$ for distances less than 15 cm from the field edge and $D_{MLC}/D_{IMRT} < 1$ for distances above 15 cm from the field edge.

From Fig. 7 b), irradiations in Krakow, the influence of energy for the same treatment modality is indicated. In all cases as energy

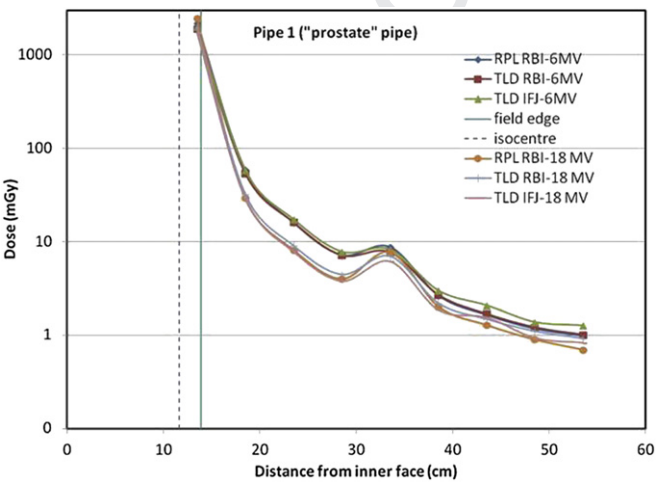

Fig. 5. Comparison of dosimeters irradiated in a BOMAB phantom by 6 and 18 MV 5-field IMRT (Krakow).

increases, the peripheral dose decreases giving D_{6MV}/D_{18MV}: 1.3–2.2 for IMRT, D_{6MV}/D_{18MV}: 1.1–1.8 for 4-field MLC and D_{6MV}/D_{18MV}: 1.1–1.3 for 1-field 10 × 10 cm^2. The equivalent results were obtained in water tank in Saclay (Bordy et al., in this issue).

The results of peripheral dose measurements are also shown in Table 3. Mean values of doses in 5 pipes (mGy per 2 Gy at isocentre ± 1 standard deviation in percent) for different modalities and for 4 distances from the field edge (isocentre) are shown. These values represent variations within slices along the longitudinal axis and also differences in out-of-field doses for different modalities. For the calculation, the mean values of 1–3 dosimeters of particular type for a given modality are used (see 3.1).

Comparison of the results in two centres for the same irradiation modalities is interesting. Two examples are shown in Fig. 8: a) for 6 MV 1-field 10 × 10 cm^2 and b) for 6 MV IMRT. The differences in peripheral doses in two centres, as expected, are small for reference 1-field 10 × 10 cm^2 with D_{Krakow}/D_{Pisa} in the range 0.9–1.1 (without the furthest point or 0.9–1.2 taking the furthest point into account). For IMRT, differences were larger, D_{Krakow}/D_{Pisa}: 1.4–1.8 (taking into account the furthest point: 1.4–2.2). The results are in agreement with the differences in treatment planning given in Fig. 9.

3.4. Comparison of TPS and dosimeters

Dose profiles from different treatment plans in Pisa and Krakow are given in Fig. 9. Distance (in cm) is given from the inner face of the posterior transverse surface of the trunk.

It is clear that the shape of the TP curves corresponds to the results of peripheral doses measured with dosimeters, but generally dosimeters show larger doses then the TPS as distance from isocentre increases. Dose distributions by TPS are given for distances up to about 15 cm from the isocentre. Beyond this distance, dosimeters show much larger doses than could be predicted by the TPS as shown for example in Fig. 10, where comparison of TPS and dosimeters for 15 MV 5-fields MLC - Pisa and 18 MV 4-fields MLC – Krakow is given. Results are for "prostate", "bladder" and "rectum" axes. The ratios of dosimeters and TPS values in the part of the curve closer to the field edge shown in Table 4 are in the range 1.15–2.25. The estimation of the sparing of adjacent sensitive organs from PTV dose data is shown in Fig. 11. Maximum doses for "bladder" (pipe 4) and "rectum" (pipe 5) as the percentage of TP dose for "prostate" (pipe 1) are given for modalities in Pisa (P) and Krakow (K). Generally doses in rectum pipe are lower than in bladder pipe, with exception of 4-field MLC in Krakow as shown in Fig. 6 and also for IMRT in Pisa. The reasons are in the beam angles applied which give the same doses in the rectum and bladder for 4-field MLC and higher doses for the rectum in case of IMRT in Pisa. The best results for sparing bladder and rectum are obtained for IMRT in both hospitals and for 5-field MLC in Pisa.

3.5. Surface – depth dose results

In Pisa, surface doses were measured for 5-field MLC, IMRT and VMAT modalities. The measured doses were compared with underlying doses within the phantom. It was assumed that mean slab dose is an adequate approximation to organ dose within the slab. The mean slab doses (with corresponding SD) for the different distances from the field edge are shown in Table 3. The results for mean pipe dose or mean surface versus distance were fitted using equation:

$$\varphi = k_0 + k_1 e^{-aD'} + k_2 e^{-bD'} + k_3 e^{-cD'} \quad (2)$$

where $\varphi(D')$ is mean surface or mean pipe dose and D' is distance from the isocentre.

Please cite this article in press as: Miljanić, S., et al., Clinical simulations of prostate radiotherapy using BOMAB-like phantoms: Results for photons, Radiation Measurements (2013), http://dx.doi.org/10.1016/j.radmeas.2012.12.012

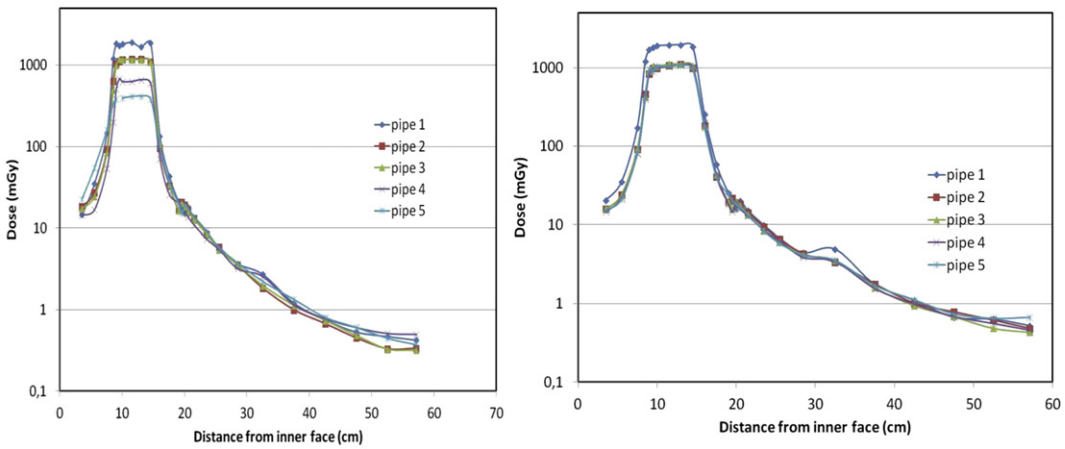

Fig. 6. Dose distribution measurements with OSL CEA dosimeters in 5 pipes; left: 5-field MLC, 15 MV, Pisa and right: 4-field MLC, 18 MV, Krakow.

Ratios of fitted mean pipe dose and mean surface dose for three different modalities are shown in Fig. 12 revealed quite different relationships for MLC, IMRT and VMAT.

4. Discussion

4.1. Comparison of dosimetry systems

The comparison of RPL and TL dosimeters under the same irradiation conditions in a water tank showed that dosimeters generally agreed to within 3% in out-of-field region compared with ion chamber reference measurements in reference clinical linac beam. For OSL, dosimeter response was corrected for spectra at different depths in water (Bordy et al., in this issue). Variation of dosimeter measurements in BOMAB-like phantoms for different modalities was larger, standard deviations ranging from 6 to 10%. The possible reason is due to the changing gantry angles during the irradiations that could influence the angular dependence of dosimeters that was not the case in 1-field irradiation under reference conditions. For RPL of the same glass dimensions as in our work, Son et al. (2011) showed that the variation of sensitivity at an angle of 0° was almost 9% lower in comparison to 90° for a 6 MV photon beam. For nanoDot OSL dosimeters (5 mm diameter disk, 0.2 mm thick) when irradiated with the incident photons beam parallel to the plane of the dosimeter, nanoDot response was 4% lower at 6 MV and 3% lower at 18 MV than the response when irradiated with the incident beam normal to the plane of dosimeter (Kerns et al., 2011). For LiF, no data on angular dependence could be found in the literature for dosimeters with dimensions used in these experiments. Neutron contribution to the dose absorbed in dosimeters could be another source of uncertainty, but according to previous published data sensitivity to neutron absorbed dose probably could be neglected. When comparing different dosimeters types at different modalities of irradiation in Figs. 5 and 6 (and in all other irradiations) one can see that there are no systematic deviations between dosimeters which suggests that energy dependence of dosimeters is well compensated (in case of RPL) well corrected (in case of OSL) and can be neglected for LiF based TLDs. In this investigation, the uncertainty in the mean dose decreases when the number of dosimeters of various types (and hence independent measurements) increases.

4.2. Components of out-of-field doses and their characteristics for different modalities

The new advances in imaging, treatment planning and delivery are providing radiation oncologists with the ability to conform dose closely to the target (tumour) volume while minimizing the dose to organs at risk. However, this transition from 2DRT to 3DCRT and/or IMRT has resulted in clear changes to the dose distribution that previous clinical experience and second malignancy studies are based on. The review by Purdy (2008) shows that in general there is

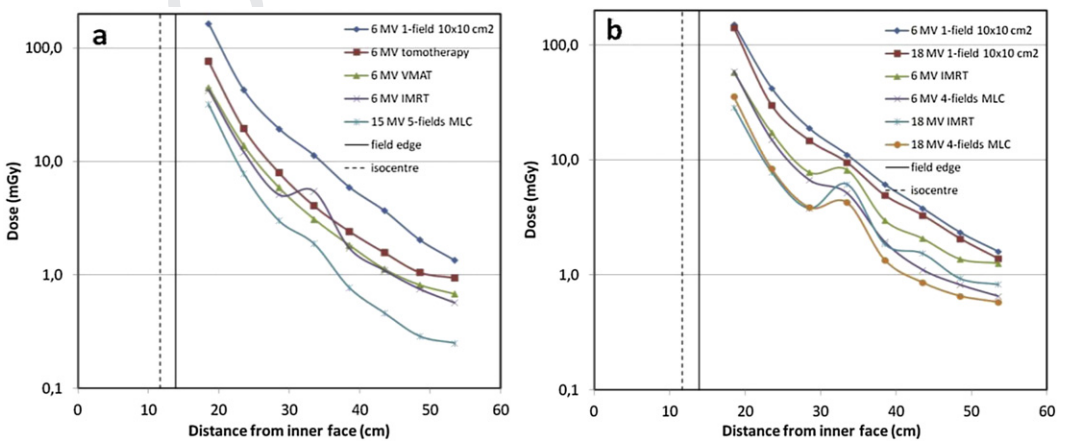

Fig. 7. Comparison of out-field-doses for different treatment modalities: a) irradiations in Pisa and b) irradiations in Krakow.

Please cite this article in press as: Miljanić, S., et al., Clinical simulations of prostate radiotherapy using BOMAB-like phantoms: Results for photons, Radiation Measurements (2013), http://dx.doi.org/10.1016/j.radmeas.2012.12.012

Table 3
Mean values of doses in 5 pipes (mGy per fraction of 2 Gy at isocentre ± standard deviation in percent) for different modalities and for different distances from the field edge (isocentre).

Distance from the field edge (isocentre) (cm)	5-Field MLC	IMRT	VMAT	Tomotherapy
	15 MV	6 MV	6 MV	6 MV
Pisa				
9.6 (11.85)	5.68 ± 36.3%	10.88 ± 6.5%	12.57 ± 5.6%	17.41 ± 6.7%
19.6 (21.85)	1.55 ± 13.6%	4.12 ± 19.7%	3.09 ± 0.89%	3.88 ± 4.0%
29.6 (31.85)	0.45 ± 2.6%	1.02 ± 7.7%	1.12 ± 4.0%	1.46 ± 6.7%
39.6 (41.85)	0.27 ± 12.8%	0.61 ± 6.6%	0.66 ± 6.3%	0.94 ± 3.8%
Distance from the field edge (isocentre) (cm)	4-field MLC	4-field MLC	IMRT	IMRT
	6 MV	18 MV	6 MV	18 MV
Krakow				
9.6 (11,85)	13.96 ± 5.1%	7.64 ± 6.1%	15.21 ± 5.6%	8.04 ± 3.8%
19.6 (21.85)	4.07 ± 15.1%	3.11 ± 21.3%	6.94 ± 12.6%	5.73 ± 13.6%
29.6 (31.85)	1.14 ± 5.7%	0.90 ± 8.9%	1.76 ± 1.9%	1.36 ± 3.7%
39.6 (41.85)	0.67 ± 2.7%	0.57 ± 5.6%	1.07 ± 2.9%	0.76 ± 17.5%

an increase in dose to the patient's target volume that includes the tumour and a limited amount of normal tissue, and an overall reduction in the volume of normal tissue receiving a high dose. However, particularly in the case of IMRT/IGRT, there is a larger volume of normal tissue that is irradiated to low radiation doses. Also compared to 2DRT and 3DCRT, IMRT requires a significantly larger number of monitor units (MUs) to deliver a comparable prescribed dose, which results in an increase in the whole body dose as a result of leakage and scattered radiation. Thus, there is some potential that this era of conformal therapy may actually result in an increased rate of secondary malignancy (Hall and Wuu, 2003). Dose deposited in a patient or phantom by X rays consists of primary and secondary components. *Primary* dose is delivered by unscattered photons and is confined to the treatment field. Kase et al. (1983) investigated the secondary radiation and their components for 3DCRT. They showed that radiation outside the treatment field arises from scatter generated by the patient (internal scatter), machine (collimator) scatter, and from leakage through the machine's shielding and collimators. They found that internal scatter can be described by a simple exponential function of distance from the central axis for all energies and field sizes. Machine scatter contributes 20–40% of total scattered dose depending on machine, field size and distance from the field. Leakage radiation contributes very little dose, but becomes dominant component at the distances beyond 60 cm from the central axis.

Ruben et al. (2011) investigated differences in scatter and leakage between 6 MV IMRT and 3DCRT to describe the relative contribution of internal patient scatter, collimator scatter and head leakage. They found that IMRT results in higher total dose to the patient than does 3DCRT. This increase is small in absolute terms and reductions in internal patient scatter with IMRT are outweighed by increased machine scatter and leakage, at least for small fields. Reductions from IMRT in dose to tissues from internal scatter, which predominates close to the field edge, means that calculations based solely on dose to distant tissues may overestimated carcinogenic risks. The relative contributions of different components of scatter and leakage are likely to vary with field size, beam energy, MU requirements of IMRT, and depth of measurements. Under conditions tested by Ruben et al. (2011) total machine scatter contributed 65% of secondary dose for IMRT but only 30% for 3DCRT. It important to point out that collimator scatter and head leakage are also dependent on linear accelerator and collimator design. Chofor et al. (2010) pointed out that any changes in beam head design, possibly capable of reducing the peripheral doses in photon therapy, have become a matter of great interest (Hall, 2006). The fraction due to body/phantom scatter is largely *unavoidable* and slightly depends on photon energy and two other contributions, are technically modifiable and therefore *avoidable*.

Numerous authors have measured out-of-field doses in several phantom designs, including water tanks and similar simple geometrical phantoms, and anthropomorphic phantoms. In an extensive review on the peripheral doses occurring in external photon-beam treatment Xu et al. (2008) reported 23 studies that considered out-of-field dose from IMRT including Tomotherapy. They summarised some out-of-field measurements for contemporary radiotherapy techniques. Outside the treatment volume at a given distance from the isocentre, out-of-field doses can vary by an order of magnitude or more, depending upon the treatment technique simulated and the linear accelerator employed. However, the methods used to derive peripheral doses differed from one author to another, making it difficult to assess the variability in peripheral dose caused by geometry of the specific linac. Joosten et al. (2011) performed measurements at five different linacs and they found that peripheral doses could differ up to a factor 9 for small fields (5×5 cm^2) and up to a factor of 10 for wedged fields.

In our work, the organs' positions and dimensions were exactly the same in both Pisa and Krakow irradiations and the main goal was to compare different modalities for the same irradiation conditions in Pisa and Krakow for the same type of linac.

The results of comparison MLC 6 MV and IMRT 6 MV (Fig. 7 and Table 4, Krakow) show that out-of-field doses for IMRT are lower

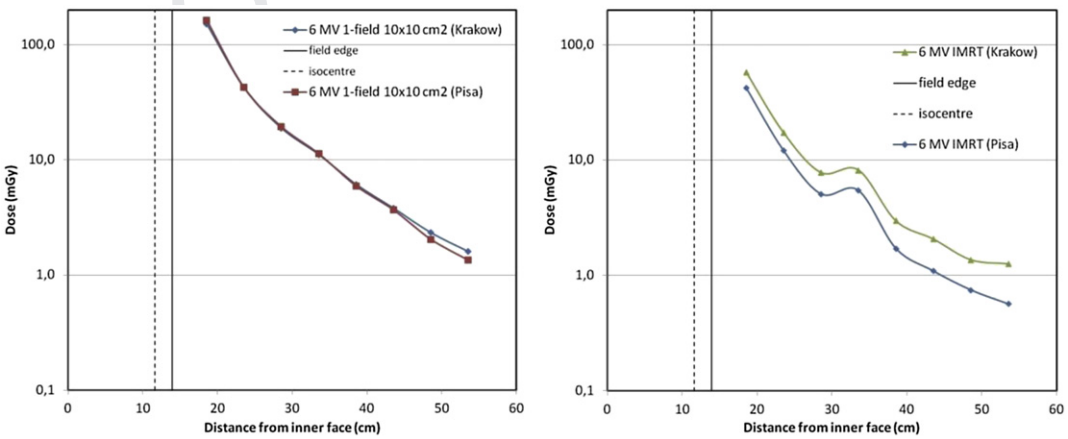

Fig. 8. Comparison of peripheral doses for the same irradiation conditions in Pisa and Krakow, for 6 MV 1-field and 6 MV IMRT.

Please cite this article in press as: Miljanić, S., et al., Clinical simulations of prostate radiotherapy using BOMAB-like phantoms: Results for photons, Radiation Measurements (2013), http://dx.doi.org/10.1016/j.radmeas.2012.12.012

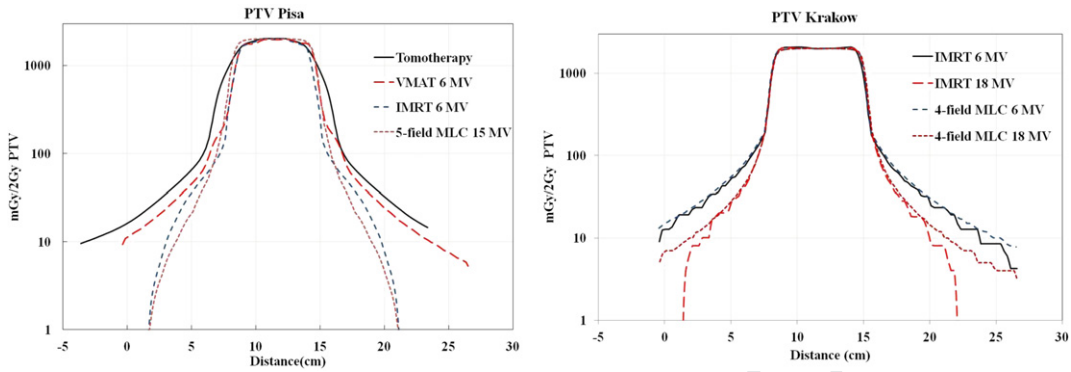

Fig. 9. Dose profiles on PTV pipe axis (pipe 1).

than that of MLC only at the distances closer to field edge (4.6 cm), they are almost the same up to 14.6 cm and after become higher for IMRT showing characteristic "bump" with maximum at about 19.6 cm. For further distances IMRT give about 50% higher doses than MLC (for doses higher than about 1 mGy). Ruben et al. (2011) also found a prominent spike in the machine scatter (largely from leakage) over a distance of 5 cm, beginning approximately 15 cm away from the edge of the field. They considered it a product of the treatment head geometry, namely, leakage radiation penetrating through the Y-yaw of the secondary collimator before passing through a gap between the lateral edge of the MLC and the primary collimator.

The comparison of the same modalities with different energies (MLC 6 MV and 18 MV; IMRT 6 MV and 18 MV) in Krakow irradiations (Fig. 7, Tables 3 and 4) shows that the peripheral photon doses are always significantly lower for higher energies. A similar finding was seen in the reference clinical linac (Saturn 43) beam in a water tank for radiation qualities of 6, 12 and 20 MV. It was found that when energy increases, water scatter decreases, collimator scatter slightly increase, leakage increases and the combined result is that total peripheral doses decrease as the energy increase (Bordy et al., in this issue). The lower photon peripheral doses from 18 MV in comparison with 6 MV photon beams equipped with MLC were obtained by Stern (1999) and Mazonakis et al. (2008). Despite the

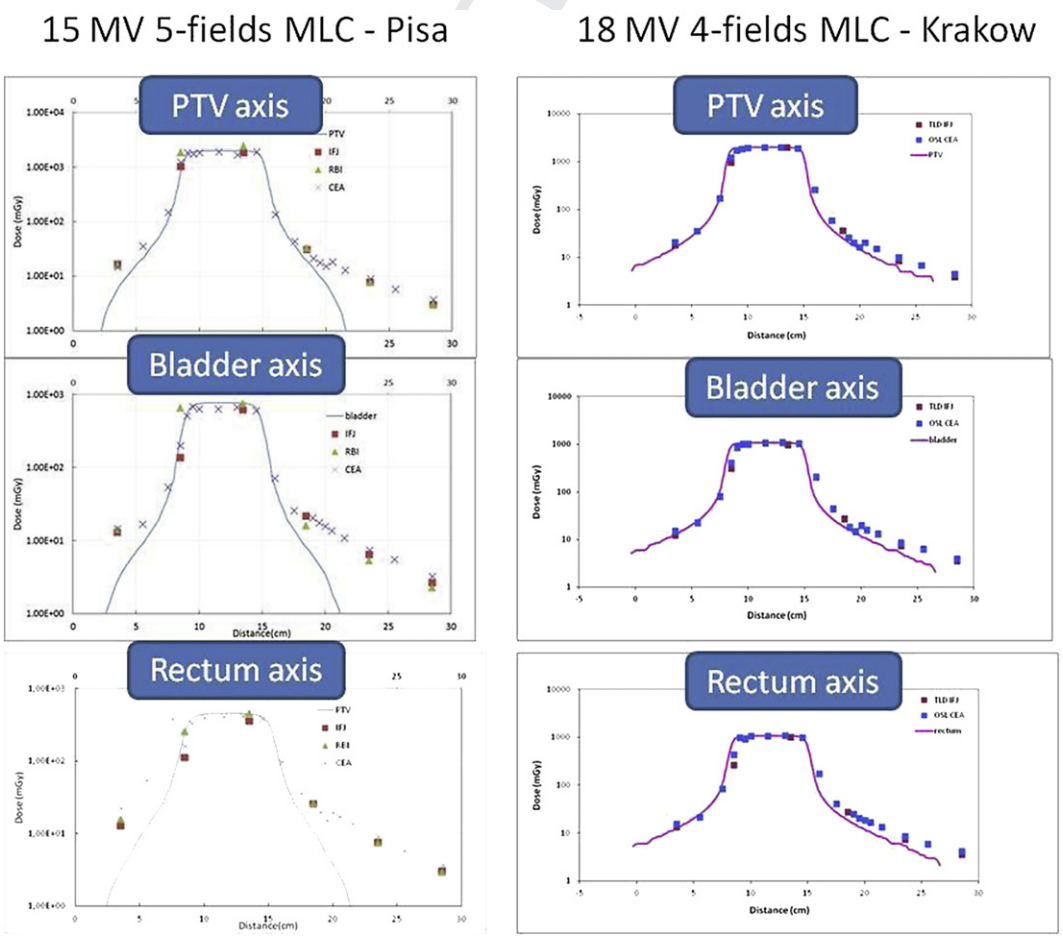

Fig. 10. Comparison of TPS and dosimeters for 15 MV 5-fields MLC - Pisa and 18 MV 4-fields MLC – Krakow – results are given for prostate, bladder and rectum axes. Q4

Please cite this article in press as: Miljanić, S., et al., Clinical simulations of prostate radiotherapy using BOMAB-like phantoms: Results for photons, Radiation Measurements (2013), http://dx.doi.org/10.1016/j.radmeas.2012.12.012

Table 4
Comparison of doses measured by dosemeters and from treatment planning for different modalities per 2 Gy at isocentre. Doses measured in Krakow using MLCs were measured with TLD IFJ and for all other modalities are mean values of RPL and TLD IFJ.

Distance from the field edge (isocentre) (cm)	5-field MLC 15 MV			IMRT 6 MV			VMAT 6 MV			Tomotherapy 6 MV		
	D_{meas} (mGy)	TPS (mGy)	D_{meas}/TPS	D_{meas} (mGy)	TPS (mGy)	D_{meas}/TPS	D_{meas} (mGy)	TPS (mGy)	D_{meas}/TPS	D_{meas} (mGy)	TPS (mGy)	D_{meas}/TPS
Pisa												
4.60 (6.85)	31.91	14.20	2.25	42.44	25.10	1.69	44.88	39.00	1.15	76.52	50.53	1.51
9.60(11.85)	7.82	/	/	12.13	/	/	13.79	10.20	1.35	19.48	/	/
Distance from the field edge (isocentre) (cm)	4-field MLC 6 MV			4-field MLC 18 MV			IMRT 6 MV			IMRT 18 MV		
	D_{meas} (mGy)	TPS (mGy)	D_{meas}/TPS	D_{meas} (mGy)	TPS (mGy)	D_{meas}/TPS	D_{meas} (mGy)	TPS (mGy)	D_{meas}/TPS	D_{meas} (mGy)	TPS (mGy)	D_{meas}/TPS
Krakow												
4.60 (6.85)	59.33	47.65	1.25	35.59	24.80	1.44	56.83	44.60	1.27	30.24	19.70	1.54
9.60(11.85)	15.10	13.10	1.15	8.42	5.68	1.48	16.48	/	/	8.38	/	/

fact that peripheral doses decrease when energy increases, there is a further controversy about the optimal energy at which to conduct IMRT (Followill et al., 2007). While high-energy therapy may offer steeper dose gradients around the planning target volume and increased skin-sparing (Followill et al., 2007), it may also lead to an increased risk of secondary malignancy due to the presence of neutrons for energies above 8 MV (Kry et al., 2005b). Kry et al. (2005a) measured out-of-field doses for 6, 10, 15 and 18 MV IMRT. They found large differences in peripheral doses between Siemens and Varian accelerators; peripheral doses were lower, but not significantly, as energy increased. In a recently published paper, Kry et al. (2009) evaluated photon and neutron out-of-field dose equivalents for 6 and 18 MV IMRT using Monte Carlo studies, and showed that there are no significant differences in second cancer risk between them. Taking into account neutron dose components, Howell et al. (2006) calculated effective dose for 6, 15 and 18 MV IMRT and found that 6 MV resulted in the lowest effective dose, while 18 MV resulted in highest effective dose.

The comparison of different modalities for irradiations in Pisa in Krakow irradiations (Fig. 7, Tables 3 and 4) shows that the highest peripheral doses were measured for Tomotherapy and somewhat less (but significantly higher than for IMRT) for VMAT.

For Tomotherapy, the beam on time needed to deliver a given prescribed dose can be up to 15 times longer than that needed using conventional treatment delivery. Because of that there is concern that this technique has the potential to increase the whole body dose due to increased scatter and leakage as found by Mutic and Low (1998), Wiezorek et al. (2009) and in our work, but despite that Ramsey et al. (2006) found the peripheral doses equal to or less than the published peripheral doses for IMRT delivery in most clinical RT applications, explaining their results by Tomotherapy delivery system designed to maximize the shielding for radiation leakage.

For VMAT modalities there are no published data on peripheral doses so far.

4.3. Characteristics of TPS calculations for different modalities and comparison with dosimeter measurements

The objective of delivering a therapeutic dose to a well-defined target while minimizing the dose to the surrounding normal tissue and critical organs requires optimization of conformity of the prescription dose to the planning target volume (PTV), dose homogeneity within the PTV, and dose to the surrounding normal tissue and critical organs. The priority of the treatment plan is to apply the maximum dose to the tumour based on constraints of surroundings organs at risk. These dose constraints are based on clinical experience and aim at minimizing side effects (normal tissue complications). Organs at risk identified for prostate cancer are bladder and rectum. Lowering the dose to these organs is an important part of the treatment planning process.

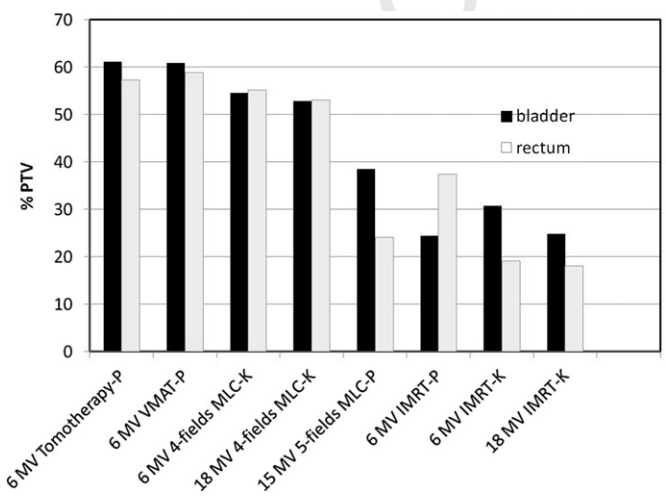

Fig. 11. Maximum doses for bladder (pipe 4) and rectum (pipe 5) as a percentage of PTV dose for prostate (pipe 1) given for modalities in Pisa (P) and Krakow (K).

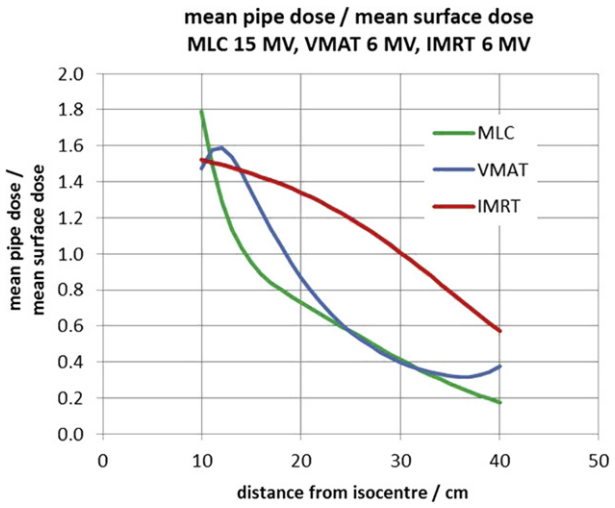

Fig. 12. Ratios of mean pipe dose and mean surface dose related to the distance from the isocentre for 5-field MLC, 6 MV VMAT and 6 MV IMRT.

Recently there have been a number of published papers dealing with comparison of 3DCRT, IMRT and novel forms of IMRT: VMAT and Tomotherapy with regard to plan qualities and treatment efficiency for prostate cancer (Aoyama et al., 2006; Palma et al., 2008; Wolff et al., 2009; Aznar et al., 2010; Zhang et al., 2010; Tsai et al., 2011) and for other cancer types (Bertelsen et al., 2010; Viellot et al., 2010; Lee et al., 2011; Lu et al., in press).

Aoyama et al. (2006) (for 5 patients) found an advantage of Tomotherapy over conventional IMRT and 3DCRT for localized prostate cancer in regard to dose sparing of rectal wall and penile bulb with a slight decrease in integral dose received by normal tissue (NTID) in comparison with 6 MV 3DCRT. Palma et al. (2008) (for 5 patients) found that variable dose rate VMAT resulted in a more favourable dose distribution than for IMRT and constant dose rate VMAT techniques, and reduced the MUs required compared with IMRT. Wolff et al. (2009) (for 9 patients) concluded that all new techniques yield treatment plans of improved quality compared to 3DCRT, with serial tomotherapy providing best OAR sparing and VMAT being most efficient treatment option in their comparison. Plans which were calculated with 3DCRT provided good target coverage but resulted in higher doses to the rectum. Aznar et al. (2010) (for 47 patients) compared RapidArc (RA) (Varian VMAT) with 5-field IMRT; RA results in improved sparing of rectum, however, at the expense of an increase in dose to the femoral heads in prostate patients. The treatment time is significantly reduced from RA (from 4.9 min with IMRT to 1.1 min for RA). Zhang et al. (2010) (for 11 patients) found that VMAT can reduce beam on time by up to 55% while maintaining dosimetric quality and is comparable to that of a standard IMRT approach. Tsai et al. (2011) (for 12 patients) found that VMAT and step-and-shoot IMRT have comparable dosimetry, but treatment efficiency is significantly higher for VMAT than for IMRT and Helical Tomotherapy (HT). HT spares more rectal volume and has better conformity, but requires the highest number of MUs. Although it requires fewer MUs than HT, step-and-shoot IMRT is the least favourable of the 3 techniques in rectal sparing.

Bertelsen et al. (2010) (for 25 patients) for head and neck cancer found that target coverage in the IMRT and VMAT plans were very similar. VMAT plans had equivalent or better target coverage and sparing of OARs than IMRT, while both delivery time and MUs were decreased. Viellot et al. (2010) showed that for 10 patients with anal canal cancer RapidArc was able to deliver an equivalent treatment plan to IMRT in terms of PTV coverage. It provided a better organ at risk sparing and significant reduction of MU ~~and treatment plan~~ per fraction. Lee et al. (2011) (18 patients with nasopharyngeal carcinoma, NPC) using SmartArc, dual arc VMAT produced plans with similar target coverage, as well as sparing OARs with 7field-IMRT. The major difference between VMAT and IMRT for a sequential mode in treating NPC appears to be improved efficiency, resulting i a faster delivery time and the use of fewer MU. Results of Lu et al. (in press) (12 patients with NPC) indicate (ha) VMAT provides better sparing of normal tissue, homogeneity, conformity than IMRT, and the same characteristics but shorter delivery time than HT.

In all the above papers it was claimed that the novel forms of IMRT (VMAT and Tomotherapy) show better treatment efficiency and usually better sparing of OARs. The most pronounced quality of VMAT is much lower MU and delivery time in comparison with conventional IMRT. In this work we compare treatment planning systems for different modalities and from two centres and their results compare with the results of dosimeters' measurements. Dose profiles for the planning target volumes for prostate in Fig. 9 show that out-of-field doses are quite different for different modalities and their order from the highest to the lowest values is the same as with dosimetry measurements shown in Fig. 7. Differences in dosimetry results in Fig. 8 between 6 MV IMRT in two centres can also be attributed to differences in TPS applied in two centres.

In Fig. 10, comparison of dosimeter readings with the TPS for OARs, bladder and rectum is shown for 3DCRT MLC for Pisa and Krakow irradiation. Dosimeters show larger values than TPS in all cases. Howell et al. (2010a) also determined that Eclipse TPS underestimated doses outside the treatment field by an average of 40% for a clinical treatment delivered on a Varian Clinac 2100. In Table 4, comparison of doses measured by dosimeters and from the TPS for different modalities per 2 Gy at isocentre is shown for distances for which comparison was possible by TPS (for further distances results for TPS are not possible). At a distance of 4.6 cm from the field edge, the ratios of doses measured by dosimeters and that from TPS vary from 1.15 up to 2.25. Accordingly out-of-field doses from TPSs should only be used with a clear understanding of the accuracy of dose calculations outside the treatment field. Whereas in-field radiation doses can be accurately and rapidly calculated using commercially available treatment planning systems, these TPSs do not, however, accurately model doses outside the treatment field, nor are they designed for such calculations. Studies that require accurate out-of-field should use other dose reconstruction methods, such as measurements or simulated phantom calculations. Measurements in phantoms are accurate over a broad range of doses and closely reproduce the irradiation of a patient. Radiation dose measurements in anthropomorphic phantoms are consider the "gold standard" in peripheral dose assessment and have frequently been used to determine peripheral organ doses in studies of radiation-induced late effects from photon radiotherapy (Howell et al., 2010b). In this study, a BOMAB like phantom was used which enables easier dose measurements with close approximation of clinical situations.

The estimation of the sparing of adjacent sensitive organs from PTV data shown in Fig. 11 are also in agreement with the shapes of the PTV curves in Fig. 9. These results contrary to the majority of above cited papers show the better results of bladder and rectum sparing for conventional IMRT techniques, than for Tomotherapy and VMAT. As a conclusion it is important to point out the importance of investigation and measurement of out-of-field doses especially for the new RT modalities.

4.4. Surface dose measurements

One possible technique for dose and risk estimates is to make surface dose measurements. The main idea is to relate surface measurements to underlying mean slab dose, then to validate relationships with BOMAB and anthropomorphic phantom measurements. The assumption is that the mean slab dose may be taken to be an adequate approximation to organ dose within the slab. Particularly at large distances from the target, where doses due to leakage and collimator scatter exceed those due to patient scatter, the circular symmetry of dose delivery will tend to reduce the variation of doses at points within an axial slab. In Table 3 the mean slab doses were calculated for certain distances from the field edge. The ratios of mean pipe (slab) doses and mean surface doses for different distances (Fig. 12) show quite different shapes for different modalities. These preliminary results need further investigation using diodes and/or passive dosimeters for surface dose measurements.

5. Conclusions

Dosimetric methods used in this study (TLD, OSL and RPL) can be used for out-of-field dosimetry. All show good uniformity, good reproducibility, and can be used down to low doses expected at distances remote from the subsequent radiotherapy target volume.

Please cite this article in press as: Miljanić, S., et al., Clinical simulations of prostate radiotherapy using BOMAB-like phantoms: Results for photons, Radiation Measurements (2013), http://dx.doi.org/10.1016/j.radmeas.2012.12.012

Comparison of TLD, OSL and RPL dosimeters under the same irradiation conditions showed that dosimeters generally agreed to within 3% compared with ion chamber reference measurements. Dosimetry measurements were performed in a BOMAB-like phantom. This phantom is more clinically realistic than a water tank, sufficiently to allow the simulation of some clinical treatments.

Comparison of out-of-field doses for different modalities in two RT centres shows that differences in out-of-field doses for the same PTV can even be a factor of 4. For sparing adjacent organs-at-risk the best results for IMRT were obtained. On the other hand, the lowest out-of-field doses were for MLC conformal therapy. Further investigations are needed especially since results revealed the fact that the TPS used, regularly underestimated out-of-field doses. Special attention should be given to the surface dose measurements as these suggest possibilities for direct dose determination during RT treatment on patients.

References

Agosteo, S., Foglio Para, A., Gerardi, F., Silari, M., Torresin, A., Tosi, G., 1993. Photoneutron dose in soft tissue phantoms irradiated by 25 MV X-rays. Phys. Med. Biol. 38, 1509–1528.

ANSI, 1995. Health Physics Society. Specifications for the Bottle Manikin Absorber Phantom. An American National Standard. American National Standards Institute, New York. ANSI/HPS N13.35; 1995.

Aoyama, H., Westerly, D.C., Rocwell, M.T., Olivera, G., Bentzen, S.M., Patel, R.R., Jaradat, H., Tome, W.A., Ritter, M.A., Mehta, M.P., 2006. Integral radiation dose to normal structures with conformal external beam radiation. Int. J. Radiat. Oncol. Biol. Phys. 64, 962–967.

Aznar, M.C., Petersen, P.M., Logadottir, A., Lindberg, H., Korreman, S.S., Kjær-Kristofersen, F., Engelholm, S.A., 2010. Rotational radiotherapy for prostate cancer in clinical practice. Radiother. Oncol. 97, 480–484.

Bertelsen, A., Hansen, C.R., Johansen, J., Brink, C., 2010. Single Arc Volumetric Arc therapy of head and neck cancer. Radiother. Oncol. 95 (2), 142–148.

Bordy, J.M., d'Agostino, E., Bessiere, I., Domingo, C., d'Errico, F., di Fulvio, A., Knežević, Ž., Miljanić, S., Olko, P., Ostrosky, A., Poumarede, B., Sorel, S., Stolarczyk, L., Vermersse D., Harrison, R. Radiotherapy out-of-field dosimetry: Experimental and computational results for photons in a water tank. Radiation Measurements, in this issue.

Bucci, M.K., Bevan, A., Roach, M., 2005. Advances in radiation therapy: conventional to 3D, to IMRT, to 4D, and beyond. CA Cancer J. Clin. 55, 117–134. © American Cancer Society, Inc.

Bush, F., 1949. The integral dose received from a uniformly distributed radioactive isotope. Br. J. Radiol. 22, 96–102.

Chofor, N., Harder, D., Rühmann, A., Wilborn, K.C., Wiezorek, T., Poppe, B., 2010. Experimental study on photon-beam peripheral doses, their components and some possibilities for their reduction. Phys. Med. Biol. 55, 4011–4027.

CRUK, 2012. Cancer Research UK [Online]. http://info.cancerresearchuk.org/cancerstats.

d'Errico, F., Di Fulvio, A., Tana, L., Domingo, C., de San Pedro, M., D'Agostino, E., Clinical simulations of prostate radiotherapy using BOMAB-like phantoms: results for neutrons. Radiat. Measurements, in this issue.

Followill, D.S., Nusslin, P., Orton, C., 2007. IMRT should not be administered at photon energies grater than 10 MV. Med. Phys. 34, 1877–1879.

Gibson, J.A.B., 1986. The relative tissue kerma sensitivity of thermoluminescent materials to neutrons. Radiat. Prot. Dosim. 15, 253–266.

Hall, E.J., 2006. Intensity-modulated radiation therapy, protons, and the risk of second cancers. Int. J. Radiat. Oncol. Biol. Phys. 65 (1), 1–7.

Hall, E.J., Wuu, C.-S., 2003. Radiation-induced second cancer: the impact of 3D-CRT and IMRT. Int. J. Radiat. Oncol. Biol. Phys. 56 (1), 83–88.

Harrison, R.M. Introduction to dosimetry and risk estimation of second cancer induction following radiotherapy. Radiat. Measurements, in this issue.

Howell, R.M., Hertel, N.E., Wang, Z., Hutchinson, J., Fullerton, G.D., 2006. Calculation of effective dose from measurements of secondary neutron spectra and scattered photon dose from dynamic MLC IMRT for 6 MV, 15 MV, and 18 MV beam energies. Med. Phys. 33 (2), 360–368.

Howell, R.M., Scarboro, S.B., Kry, S.F., Yaldo, D.Z., 2010a. Accuracy of out-of-field dose calculations by a commercial treatment planning system. Phys. Med. Biol. 55, 6999–7008.

Howell, R.M., Scarboro, S.B., Taddei, P.J., Krishnan, S., Kry, S.F., Newhauser, W.D., 2010b. Methodology for determining doses to in-field, out-of-field and partially in-field organs for late effects studies in photon radiotherapy. Phys.Med.Biol. 55, 7009–7023.

IAEA, 2000. Absorbed Dose Determination in External Beam Radiotherapy. An International Code of Practice for Dosimetry Based on Standards of Absorbed Dose to Water. Technical Reports Series No. 398. International Atomic Energy Agency, Vienna.

IAEA, 2008. Transition from 2-D Radiotherapy to 3-D Conformal and Intensity Modulated Radiotherapy. IAEA-TECDOC-1588. IAEA, Vienna.

ICRU, 1984. Neutron Dosimetry for Biology and Medicine. Report 26. ICRU Publications, Bethesda, MD.

Joosten, A., Bochud, F., Baechler, S., Levi, F., Mirimanoff, R.-O., Moeckly, R., 2011. Variability of a peripheral dose among various linac geometries for second cancer risk assessment. Phys. Med. Biol. 56, 5131–5151.

Kase, K.R., Svensson, G.K., Wolbarst, A.B., Marks, M.A., 1983. Measurements of dose from secondary radiation outside a treatment field. Int. J. Radiat. Oncol. Biol. Phys. 9 (8), 1177–1183.

Kerns, J.R., Kry, S.F., Sahoo, N., Followill, D.S., Ibbott, G.S., 2011. Angular dependence of the nanoDot OSL dosimeter. Med. Phys. 38 (7), 3955–3962.

Knežević, Ž., Stolarczyk, L., Bessiere, I., Bordy, J.M., Miljanić, S., Olko, P. Photon dosimetry methods: optically stimulated luminescence (OSL), thermoluminescence (TL) and radiophotoluminescence (RPL) dosimetry. Radiat. Measurements, in this issue.

Krpan, K., Miljanić, S., Vekić, B., Deme, S., Szántó, P., Pázmándi, T., 2008. TL and PTTL of TLD-100 and TLD-700 after irradiation with Pu–Be neutrons. Radiat. Meas. 43, 1123–1127.

Kry, S.F., Salehpour, M., Followill, D.S., Stovall, M., Kuban, D.A., White, R.A., Rosen, I.I., 2005a. Out-of-field photon and neutron dose equivalents from step-and-shoot intensity-modulated radiation therapy. Int. J. Radiat. Oncol. Biol. Phys. 62 (4), 1204–1216.

Kry, S.F., Salehpour, M., Followill, D.S., Stovall, M., Kuban, D.A., White, R.A., Rosen, I.I., 2005b. The calculated risk of fatal secondary malignancies from intensity-modulated radiation therapy. Int. J. Radiat. Oncol. Biol. Phys. 62 (4), 1195–1203.

Kry, S.F., Titt, U., Followill, D., Pönisch, F., Vassiliev, O.N., White, R.A., Stovall, M., Salehpour, M., 2007. A Monte Carlo model for out-of-field dose calculation from high-energy photon therapy. Med. Phys. 34 (9), 3489–3499.

Kry, S.F., Salehpour, M., Titt, U., White, R.A., Stovall, M., Followill, D.S., 2009. Monte Carlo study show no significant difference in second cancer risk between 6- and 18-MeV intensity modulated radiation therapy. Radiother. Oncol. 91, 132–137.

Lee, T.-F., Chao, P.-J., Ting, H.-M., Lo, S.-H., Wang, Y.-W., Tuan, C.-C., Fang, F.-M., Su, T.-J., 2011. Comparative analysis of SmartArc-based dual arc volumetric-modulated arc radiotherapy (VMAT) versus intensity-modulated radiotherapy (IMRT) for nasopharyngeal carcinoma. J. Appl. Clin. Med. Phys. 12 (4), 158–174.

Liu, H.-M., Hsu, P.-C., Liaw, T.-F., 2001. Gamma dose measurements in a water phantom irradiated with the BNCT facility at THOR. Radiat. Prot. Dosim. 95 (4), 353–358.

Lu, S.-H., Cheng, J.C.-H., Kuo, S.-H., Lee, J.J.-S., Chen, L.-H., Wu, J.-K., Chen, W.-Y., Chong, F.-C., Wu, C.-J., Wang, C.-W., Volumetric modulated arc therapy for nasopharyngeal carcinoma: a dosimetric comparison with TomoTherapy and step-and-shoot IMRT. Radiother. Oncol. in press.

Mackie, T.R., Holmes, T., Swerdloff, S., 1993. Tomotherapy: a new concept for the delivery of conformal radiotherapy. Med. Phys. 20, 1709–1719.

Mazonakis, M., Zacharopoulou, F., Varveris, H., Damilakis, J., 2008. Peripheral dose measurements for 6 and 18 MV photon beams on a linear accelerator with multileaf collimator. Med. Phys. 35 (10), 4396–4403.

Miljanić, S., Krpan, K., Blagus, S., 2007. TL and PTTL of TLD-100 and TLD-700 after irradiation with 14.5 MeV neutrons. Nucl. Instrum. Methods Phys. Res. A 574, 510–517.

Miljanić, S., Ranogajec-Komor, M., Blagus, S., Pálfalvi, J.K., Pázmándi, Pázmándi T., Deme, S., Szántó, P., 2008. Response of radiophotoluminescent dosimeters to neutrons. Radiat. Meas. 43, 1068–1071.

Mutic, S., Low, D.A., 1998. Whole-body dose from tomotherapy delivery. Int. J. Radiat. Oncol. Biol. Phys. 42 (1), 229–232.

Otto, K., 2008. Volumetric modulated arc therapy: IMRT in a single gantry arc. Med. Phys. 35, 310–317.

Palma, D., Vollans, E., James, K., Nakano, S., Moiseenko, V., Shaffer, R., McKenzie, M., Morris, J., Otto, K., 2008. Volumetric modulated arc therapy for delivery of prostate radiotherapy: comparison with intensity-modulated radiotherapy and three-dimensional radiotherapy. Int. J. Radiat. Oncol. Biol. Phys. 72 (4), 996–1001.

Pardo-Montero, J., Fenwick, J.D., 2009. An approach to multiobjective optimization of rotational therapy. Med. Phys. 36, 3292–3303.

Purdy, J., 2008. Dose to normal tissue outside the radiation therapy patient's treated volume: a review of different radiation therapy techniques. Health Phys. 95 (5), 666–676.

Ramsey, C.R., Seibert, R., Mahan, S.L., Desai, D., Chase, D., 2006. Out-of-field dosimetry measurements for a helical tomotherapy system. J. Appl. Clin. Med. Phys. 7 (3), 1–11.

Ruben, J.D., Lancaster, C.N., Jones, P., Smith, R.L., 2011. A comparison of out-of-field dose and its constituent components for intensity-modulated radiation therapy versus conformal radiation therapy: implications for carcinogenesis. Int. J. Radiat. Oncol. Biol. Phys. 81, 1458–1464.

Sawakushi, G.O., Yukihara, E.G., McKeever, S.W.S., Benton, E.R., Gaza, R., Uchihori, Y., Yasuda, N., Kitamura, H., 2008. Relative optically stimulated luminescence and thermoluminescence efficiencies of Al_2O_3:C dosimeters to heavy charged particles with energies relevant to space and radiotherapy dosimetry. J. Appl. Phys. 104, 124903–124911-10.

Son, K., Jung, H., Shin, S.H., Lee, H.-H., Kim, M.-S., Ji, Y.H., Kim, K.B., 2011. Evaluation of the dosimetric characteristics of a radiophotoluminescent glass dosimeter for high-energy photon and electron beams in the field of radiotherapy. Radiat. Merasurements 46, 1117–1122.

Stern, R.L., 1999. Peripheral dose from a linear accelerator equipped with multileaf collimation. Med. Phys. 26 (4), 559–563.

Tsai, C.-L., Wu, J.-K., Chao, H.-L., Tsai, Y.-C., Cheng, J.C.-H., 2011. Treatment and dosimetric advantages between VMAT, IMRT, and helical tomotherapy in prostate cancer. Med. Dosim. 36, 264–271.

Please cite this article in press as: Miljanić, S., et al., Clinical simulations of prostate radiotherapy using BOMAB-like phantoms: Results for photons, Radiation Measurements (2013), http://dx.doi.org/10.1016/j.radmeas.2012.12.012

Vanhavere, F., Huyskens, D., Struelens, L., 2004. Peripheral neutron and gamma doses in radiotherapy with an 18 MV linear accelerator. Radiat. Prot. Dosim. 110, 607–612.

Viellot, S., Azria, D., Lemanski, C., Moscardo, C.L., Gourgou, S., Dubois, J.-B., Aillères, N., Fenoglietto, P., 2010. Plan comparison of volumetric arc therapy (RapidArc) and conventional intensity-modulated radiation therapy (IMRT) in anal canal cancer. Radiat. Oncol. 5, 92.

Wiezorek, T., Schwahofer, A., Schubert, K., 2009. The influence of different IMRT techniques on the peripheral dose – a comparison between sMLM and helical tomotherapy. Strahlentherapie und Onkologie 185, 696–702.

Wolff, D., Stieler, F., Welzel, G., Lorenz, F., Abo-Madyan, Y., Mai, S., Polednik, M., Steil, V., Wenz, F., Lohr, F., 2009. Volumetric modulated arc therapy (VMAT) vs. serial tomotherapy, step-and shoot IMRT and 3D-conformal RT for treatment of prostate cancer. Radiother. Oncol. 93, 226–233.

Xu, X.G., Bednarz, B., Paganetti, H., 2008. A review of dosimetry studies on external-beam radiation treatment with respect to second cancer induction. Phys. Med. Biol. 53, R193–R241.

Zhang, P., Happersett, L., Hunt, M., Jackson, A., Zelefsky, M., Mageras, G., 2010. Volumetric modulated arc therapy: planning and evaluation for prostate cancer cases. Int. J. Radiat. Oncol. Biol. Phys. 76, 1456–1462.

Please cite this article in press as: Miljanić, S., et al., Clinical simulations of prostate radiotherapy using BOMAB-like phantoms: Results for photons, Radiation Measurements (2013), http://dx.doi.org/10.1016/j.radmeas.2012.12.012